Surgical Endoscopy (2019) 33:1988–1997
https://doi.org/10.1007/s00464-018-6512-6

2018 SAGES ORAL

Discrimination between arterial and venous bowel ischemia by computer-assisted analysis of the fluorescent signal

Giuseppe Quero[1] · Alfonso Lapergola[2] · Manuel Barberio[1] · Barbara Seeliger[1] · Paola Saccomandi[1] · Ludovica Guerriero[1] · Didier Mutter[1,2,3] · Alend Saadi[4] · Marc Worreth[4] · Jacques Marescaux[1,2] · Vincent Agnus[2] · Michele Diana[1,2,3,4]

Received: 27 July 2018 / Accepted: 11 October 2018 / Published online: 16 October 2018

Abstract

Background Arterial blood supply deficiency and venous congestion both play a role in anastomotic complications. Our aim was to evaluate a software-based analysis of the fluorescence signal to recognize the patterns of bowel ischemia.

Methods In 18 pigs, two clips were applied on the inferior mesenteric artery (group A: $n=6$) or vein (group V: $n=6$) or on both (group A–V: $n=6$). Three regions of interest (ROIs) were identified on the sigmoid: P = proximal to the first clip; C = central, between the two clips; and D = distal to the second clip. Indocyanine Green was injected intravenously. The fluorescence signal was captured by means of a near-infrared laparoscope. The time-to-peak (seconds) and the maximum fluorescence intensity were recorded using software. A normalized fluorescence intensity unit (NFIU: 0-to-1) was attributed, using a reference card. The NFIU's over-time variations were computed every 10 min for 50 min. Capillary lactates were measured on the sigmoid at the 3 ROIs. Various machine learning algorithms were applied for ischemia patterns recognition.

Results The time-to-peak at the ischemic ROI C was significantly longer in group A versus V (20.1 ± 13 vs. 8.43 ± 3.7; $p=0.04$) and in group A–V versus V (20.71 ± 11.6 vs. 8.43 ± 3.7; $p=0.03$). The maximal NIFU at ROI C, was higher in the V group (1.01 ± 0.21) when compared to A (0.61 ± 0.11; $p=0.002$) and A–V (0.41 ± 0.2; $p=0.0005$). Capillary lactates at ROI C were lower in V (1.3 ± 0.6) than in A (1.9 ± 0.5; $p=0.0071$), and A–V (2.6 ± 1.5; $p=0.034$). The K nearest neighbor and the Linear SVM algorithms provided both an accuracy of 75% in discriminating between A versus V and 85% in discriminating A versus A–V. The accuracy dropped to 70% when the ML had to identify the ROI and the type of ischemia simultaneously.

Conclusions The computer-assisted dynamic analysis of the fluorescence signal enables the discrimination between different bowel ischemia models.

Keywords Fluorescence angiography · Fluorescence-based Enhanced Reality · Computer-assisted analysis of fluorescence signal · Tissue perfusion · Machine learning

Fluorescence angiography (FA) enables intra-operative imaging of tissue perfusion and viability [1]. FA is based on the use of near-infrared camera systems that capture the excitation signal of a systemically injected fluorophore, most often Indocyanine Green (ICG). The proof of perfusion is provided by the presence of a fluorescent signal, witnessing of the diffusion of the fluorophore from the bloodstream to the tissue surface.

When applied to digestive surgery, FA is being investigated as a potential tool to reduce the risk of anastomotic complications, in both upper- and lower-GI resections [2], by supporting the subjective clinical estimation of the perfusion status with enhanced information.

This work was partly presented during the Instrumentation/Devices/Technologies Session (S054) at the 16th World Congress of Endoscopic Surgery, jointly hosted by SAGES & CAGS held in Seattle, WA, April 11–14, 2018.

✉ Michele Diana
michele.diana@ircad.fr; michele.diana@ihu-strasbourg.eu

1 IHU-Strasbourg, Institute of Image-Guided Surgery, 1, Place de l'Hôpital, 67091 Strasbourg, France

2 IRCAD, Research Institute against Cancer of the Digestive System, Strasbourg, France

3 Department of General, Digestive and Endocrine Surgery, University Hospital of Strasbourg, Strasbourg, France

4 Department of General Surgery, Hospital of Pourtalès, Neuchâtel, Switzerland

In a recent systematic review and meta-analysis of non-randomized trials, the authors have reported a lower rate of anastomotic leaks in FA-guided when compared to clinically-guided colorectal resections [3]. Promising results are also being obtained in FA-guided construction of the gastric conduit during esophagectomy [4].

Additionally, FA can provide information about bowel viability and an image-based strategy related to the need and the extent of bowel resection [5, 6].

However, current FA studies only rely on the presence of a fluorescent signal on the target tissue, without taking into account the dynamics of the signal. ICG can diffuse over time outside of the marginal zones towards the ischemic areas and this diffusion can lead to a subjective overestimation of the perfused area. In other words, the relevant information provided by FA about the arterial vascular supply is limited to the first seconds after the injection of the fluorophore, as an angiography effect.

In order to provide a quantitative and reproducible evaluation of the dynamics of the ICG fluorescence signal, an accurate, computer-assisted method, defined as FLuorescence-based Enhanced Reality (FLER) has been introduced [7–11]. The FLER software creates a color-coded virtual perfusion cartography representing the slope of the time-to-peak of fluorescence pixel-by-pixel. The virtual cartography storing the dynamic angiography effect is overlaid onto real-time operative images to directly provide the perfusion data on the tissue.

In reconstructive and transplant surgery, the viability of the flap/graft is dependent not only on the arterial inflow but also on the venous outflow. As an example, venous congestion is the main risk factor for flap failure and the ability to identify a venous outflow deficiency could lead to performing salvage procedures [12].

In GI surgery, the possibility to discriminate between an arterial inflow and a venous outflow impairment could be relevant in the various esophageal reconstruction methods, involving the pull-up of the replacement conduits, often suffering from venous congestion [13].

In the emergency setting of acute bowel ischemia, an intraoperative FA enabling the discrimination between an arterial and a venous origin might also provide support to the surgical management [5, 6, 14].

The aim of this experimental study was to evaluate the ability of a software-based analysis of the fluorescence signal, including a machine learning (ML) approach, to identify the patterns of different forms of bowel ischemia.

Materials and methods

Animals

A total of 18 adult swine (*Sus scrofa domesticus*, ssp. Large white; 11 males and 7 females; mean weight 45.4 ± 8.85 kg) were involved in this non-survival study. The present experimental study is part of the ELIOS project (Endoscopic Luminescent Imaging for Oncology Surgery) which received full approval from the local Ethical Committee on Animal Experimentation (ICOMETH no. 38.2016.01.085), and by the French Ministry of Superior Education and Research (MESR) under the reference APAFIS #8721-2017013010316298 v2. All animals used in the experimental laboratory were managed according to French laws for animal use and care and according to the directives of the European Community Council (2010/63/EU) and the ARRIVE guidelines [15]. The animals were fasted for 24 h with free access to water before surgery. Animals were premedicated, 10 min before surgery, by means of an intramuscular injection of ketamine (20 mg/kg) and azaperone (2 mg/kg) (Stresnil; Janssen-Cilag, Belgium). Intravenous propofol (3 mg/kg) combined with rocuronium (0.8 mg/kg) were used for induction. Anesthesia was maintained with 2% isoflurane. At the end of the procedures, pigs were sacrificed with an intravenous injection of a lethal dose of potassium chloride.

Surgical procedure

A Veress needle was used to establish the pneumoperitoneum. A near-infrared optimized laparoscope (D-Light-P; Karl Storz, Tuttlingen; Germany), was inserted through a 10 mm port and two additional 10 mm ports were placed in the hypogastric and right flank regions. The sigmoid colon was exposed and suspended to the abdominal wall. The animals were randomly divided into three groups, of six animals each, according to the type of ischemia model, as follows:

1. Arterial ischemia by clipping the inferior mesenteric artery (IMA) (group A; $n = 6$);
2. Venous ischemia, by clipping the inferior mesenteric vein (IMV) (group V: $n = 6$)
3. Mixed ischemia, by clipping both the IMA and IMV (group A–V: $n = 6$).

The segmental vascular occlusion was made by the means of two clips applied 5 cm apart, on each vessel. The colon wall was divided macroscopically in three main regions of interest (ROIs), following the cranio-caudal orientation (and not the vascular flow), as follows:

1. Proximal to the first clip (P);
2. Central zone, between the two clips (C);
3. Distal to the second clip (D).

Fluorescence-based enhanced reality (FLER) based on the slope of the time-to-peak of fluorescence

After completion of the ischemia models, the laparoscope was fixed to an articulated arm, in order to stabilize the image and enable repetitive assessments. A calibration aid, providing a constant fluorescence signal (Green Balance™ ICG Reference Card; Diagnostic Green; Aschheim–Dornach; Germany), was placed in the abdominal cavity, close the bowel, to provide a reference fluorescence value. A ruler was also introduced in the cavity. In order to acquire the fluorescence signal, the camera system was switched to near-infrared mode and the shutter was set to a fixed ratio of 1/50. A bolus of ICG (Infracyanine®, Serb laboratories; Paris; France) at a dose of 0.2 mg/kg was administered intravenously, followed by a flush with 10 mL of saline. The fluorescence signal was analyzed using the ER-PERFUSION software, which enables to construct a virtual perfusion cartography of the perfusion, based on the slope of the time-to-peak for the fluorescence signal to reach the maximum intensity in a specific area (in seconds). This value is average on the recorded video for 40 s at the speed of five frames per second. The virtual perfusion cartography is consequently overlapped onto the laparoscopic images, providing the FLER (Figs. 1, 2, 3).

Over-time evolution of the fluorescence signal (wash-out) and the normalized fluorescence intensity unit

The ER-PERFUSION software was also used to analyze the evolution of the fluorescence intensity on the bowel. The maximum bowel fluorescence intensity was recorded within the first minute and a normalized fluorescence intensity unit (NIFU; 0–1) was attributed as a ratio between the fluorescence of the different ROIs of the bowel (P, C and D). The evolution of the NIFU of the same ROIs was evaluated (without any further injection of the fluorophore) every 10 min for a total duration of 50 min.

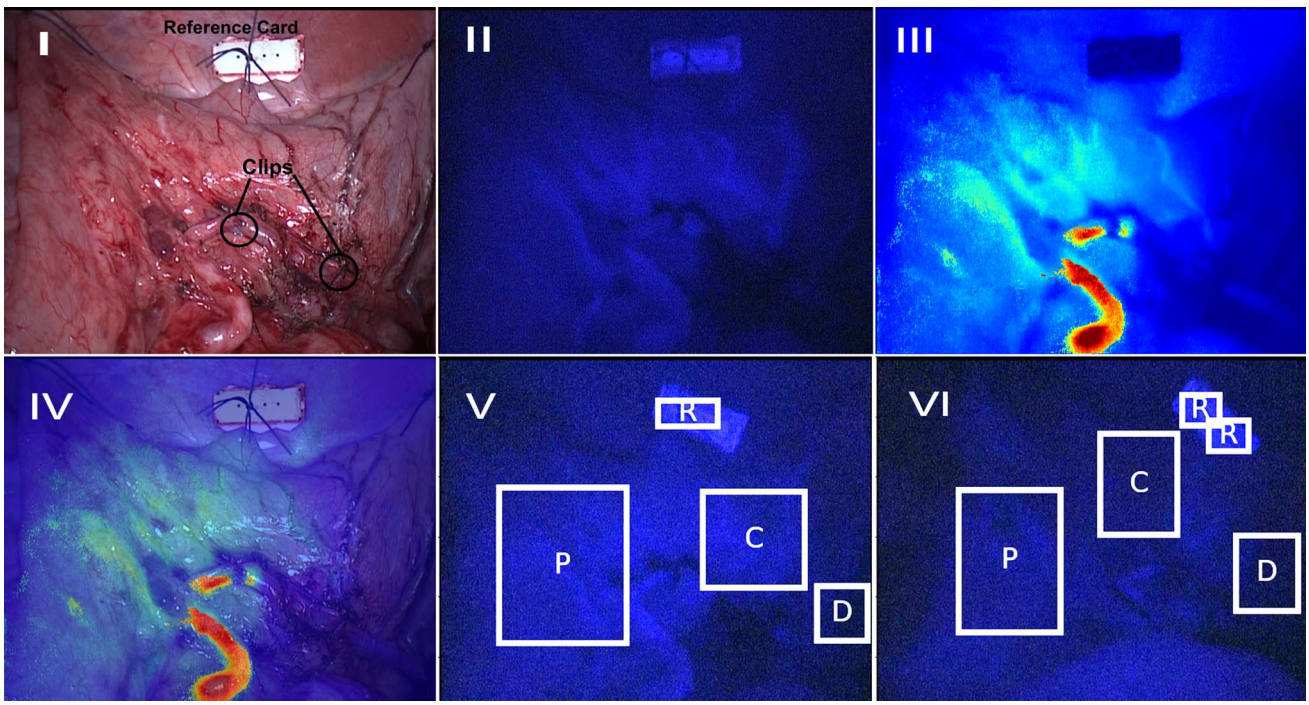

Fig. 1 Example of FLER analysis in an arterial ischemia model. **I** White light image of the minimally-invasive setting of arterial ischemia creation. The sigmoid was exposed and suspended to the abdominal wall. The inferior mesenteric artery was clipped proximally and distally, 5 cm apart. A reference card, yielding a constant fluorescent signal was placed in the abdominal cavity, close to the bowel. **II** Near-infrared image 40 s after the injection of 0.2 mg/kg of ICG: bright enhancement of the bowel vessels. **III** Virtual perfusion cartography, generated by computing the slope of the time-to-peak, pixel-by-pixel. **IV** FLER, showing the limits between the perfused proximal area (P) and the ischemic ROI C. **V** Near-infrared image after 10 min: the signal in the C area begins to rise due to the diffusion from the P area. Note the homogenous diffusion of the fluorescence signal on the bowel wall. **VI** Near-infrared image after 50 min: wash out of the signal

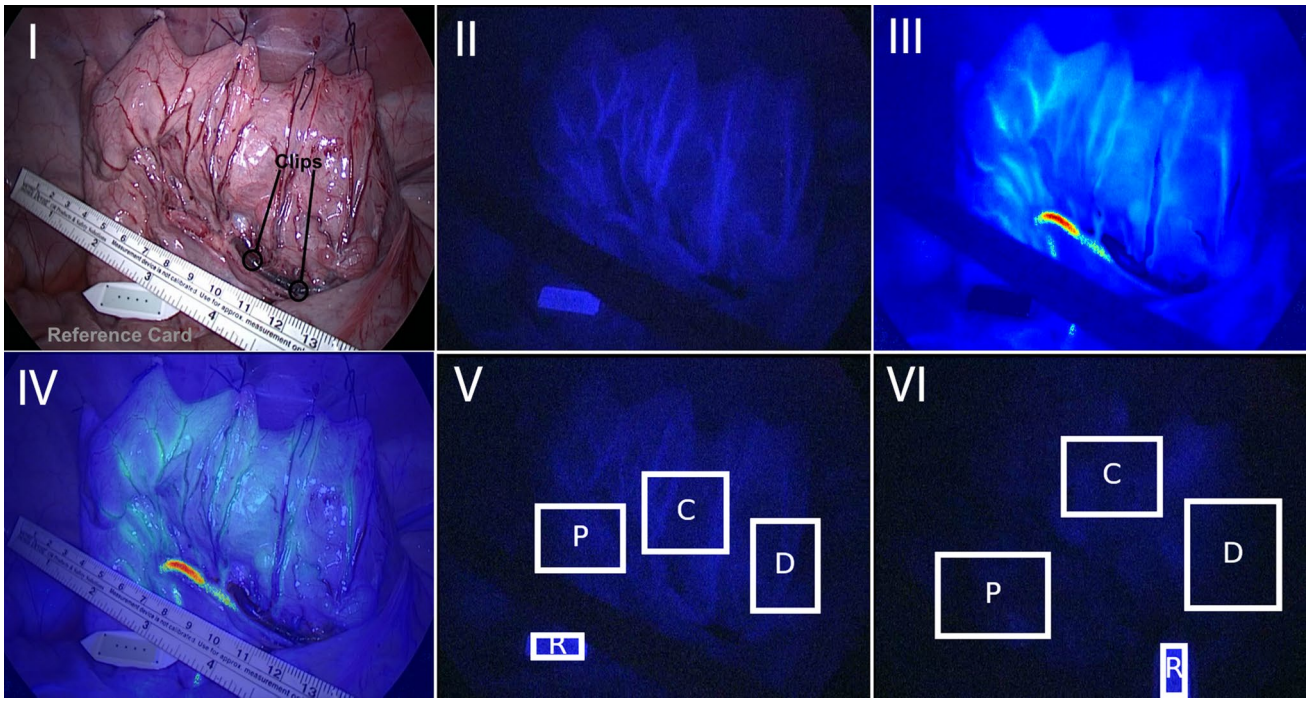

Fig. 2 Example of FLER analysis in a venous ischemia model. **I** White light image of the minimally-invasive setting of venous ischemia creation. **II** Near-infrared image 40 s after the injection of 0.2 mg/kg of ICG: brighter enhancement of the bowel vessels and homogenous enhancement of the bowel wall. **III** Virtual perfusion cartography, generated by computing the slope of the time-to-peak, pixel-by-pixel. **IV** FLER, showing a homogenous signal with no demarcation between the ROIs. **V** Near-infrared image after 10: the signal in the C remains high. **VI** Near-infrared image after 50 min: wash out of the signal, more pronounced at P and D ROIs

Local capillary lactates

Local capillary lactates were measured in the blood obtained by puncturing the bowel's serosa at the ROIs (P, C and D), 5 min after the ischemic model creation and 50 min later. The blood was aspired using a Falcon tube mounted on a motorized pipette that was introduced through one of the operating ports and then dropped on the strips of the EDGE™ blood lactate analyzer (Apex Biotechnology Corp, Taiwan; ROC), as previously described [16, 17].

Machine learning analysis

Several ML algorithms were tested to discriminate between the different ischemia models, based on the time-to-peak and the wash-out behavior of the fluorescence signal at the different time points, as follows:

1. Gradient boosting;
2. K neighbor;
3. Linear support vector machine (SVM);
4. Random forest.

Those algorithms are available for free at the scikit learn library (http://scikit-learn.org) [18].

In order to evaluate the most accurate algorithm, a cross-validation was performed using the technique of the "leave-one-out cross validation" (Devijver and Kittler [19]). In a nutshell, a single dataset is removed and the ML is trained on the remaining datasets, and tested later if the left-out dataset can be correctly "predicted" and attributed to the correct group. The operation is repeated in a loop, in order for each dataset to be left out and for the final resulting accuracy to be the mean of all the "leave-one-out" accuracies.

Statistical analysis

Except for the ML analysis, remaining statistics and graphs were obtained using the Graph Pad Prism version 6.07. The ANOVA followed by Dunnet's multiple comparison test were used to measure differences between continuous variables. A two-tailed Pearson rho coefficient was calculated to measure the correlation between variables. A p value < 0.05 was considered statistically significant.

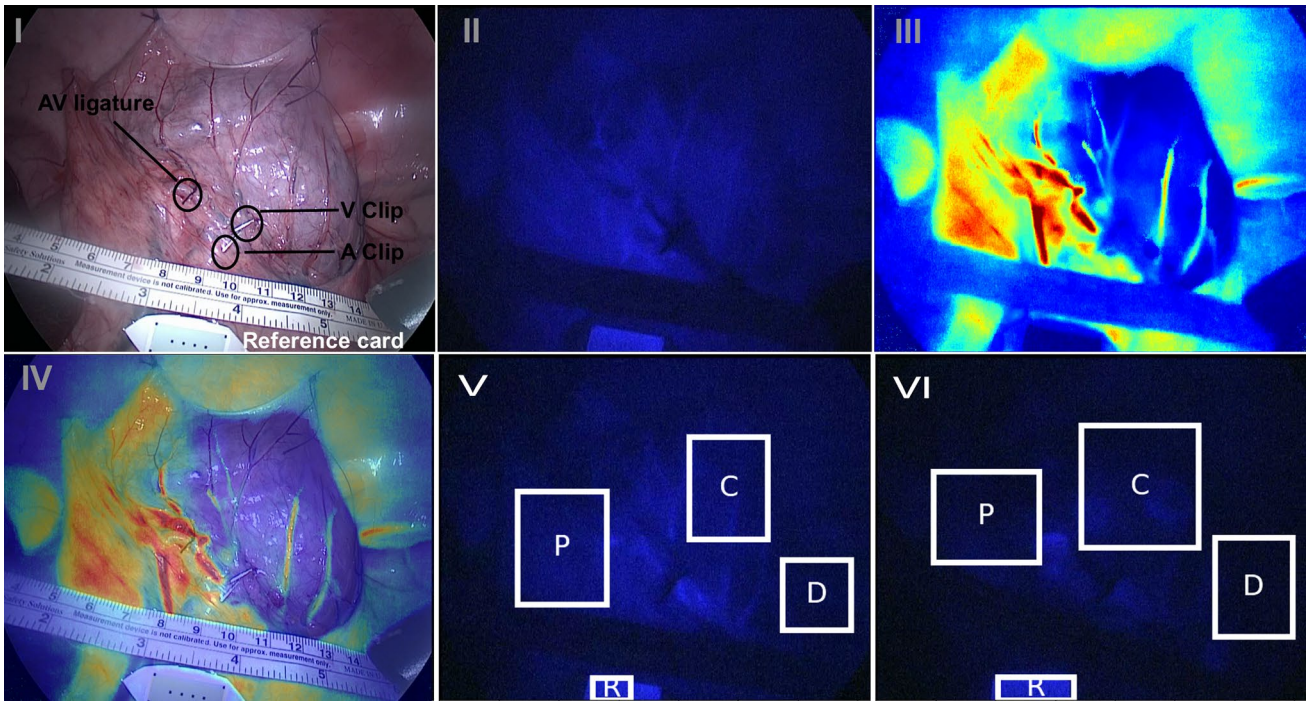

Fig. 3 Example of FLER analysis in a mixed ischemia model. **I** White light image of the minimally-invasive setting of mixed ischemia creation. **II** Near-infrared image 40 s after the injection of 0.2 mg/kg of ICG: mild enhancement of the bowel vessels. **III** Virtual perfusion cartography, generated by computing the slope of the time-to-peak, pixel-by-pixel. **IV** FLER, showing a clear demarcation of the ischemic ROI C. **V** Near-infrared image after 10 min: the signal in the C rises slightly. **VI** Near-infrared image after 50 min: homogenous wash out of the signal

Results

Slope of the time-to-peak (seconds)

The results of the slope of the time-to-peak in the various ROIs in the three different ischemia models are reported in Fig. 4.

Normalized intensity fluorescence unit (ratio between the reference card intensity and the fluorescence signal on the bowel wall; 0–1)

At the central ischemic ROI, the maximal NIFU during the first minute after the injection of the ICG, was statistically significantly higher in the V group (1.01 ± 0.21) when compared to both the A (0.61 ± 0.11; $p = 0.002$) and to the A–V group (0.41 ± 0.2; $p = 0.0005$). Similar results in terms of maximal NIFU were observed at the proximal ROI ($V = 0.82 \pm 0.07$ vs. $A = 0.6 \pm 0.2$; $p = 0.029$; vs. $A–V = 0.48 \pm 0.09$; $p < 0.0001$). At the distal ROI, maximal NIFU was also higher in the V group (0.74 ± 0.2) when compared to A (0.52 ± 0.14; $p = 0.03$) and to A–V (0.32 ± 0.11; $p = 0.0015$).

The results of the evolution of the signal due to the washout of the fluorophore are reported in Fig. 5.

Local bowel capillary lactates (mmol/L)

The results of the local bowel capillary lactates are reported in Fig. 6. There was a positive correlation between lactate levels collected at 50′ after the ischemia and the slope of the time-to-peak in case of both arterial ischemia (Pearson ρ 0.78), and venous ischemia (Pearson ρ 0.88), while no correlation was found in case of mixed ischemia (Pearson ρ 0.54).

Machine learning (ML) analysis

The most accurate algorithms to discriminate the type of ischemia, taking into account the slope of the time-to-peak, the maximum fluorescence signal at 1 min and the over-time evolution at 10–50 min, were the *K* Neighbor and the Linear SVM. When the ML was asked to recognize only the type of ischemia, independently from the ROI, the K nearest neighbor and the Linear SVM algorithms both provided an accuracy of 75% in discriminating between A versus V and 85% in discriminating A versus A–V. The accuracy dropped to 70% when the ML had to simultaneously identify the ROI and the type of ischemia.

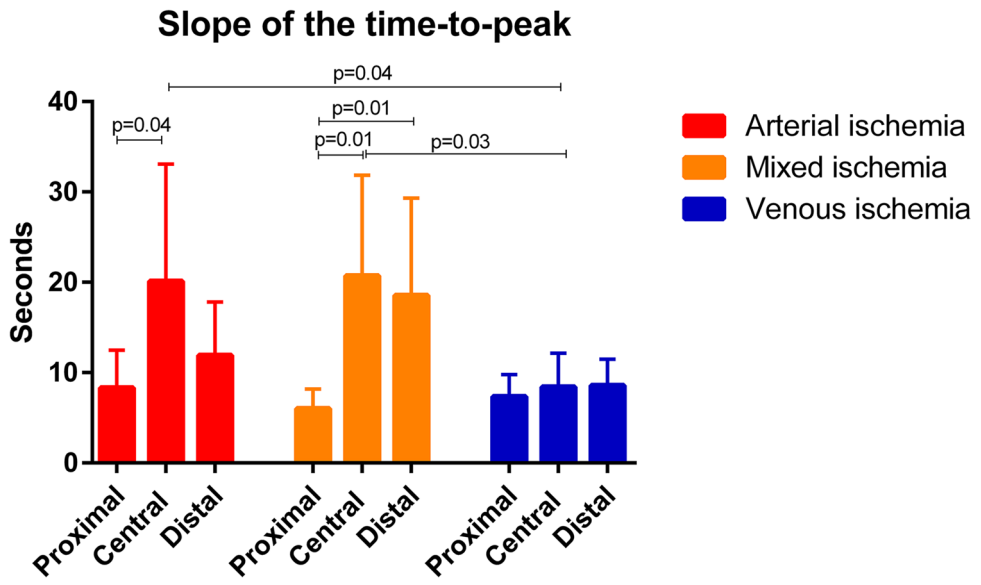

Fig. 4 Slope of the time-to-peak (seconds). In group A, the time-to-peak recorded at the ROI P (8.32 ± 4.16) was significantly shorter when compared to C (20.1 ± 13; $p = 0.04$). Similarly, in group A–V, the time-to-peak was shorter at the ROI P (6.03 ± 2.17) when compared to C (20.71 ± 11.6; $p = 0.01$) and when compared to D (18.56 ± 10.75; $p = 0.01$). In group V, the time-to-peak was similar in the three ROIs ($p = 7.35 \pm 2.43$; C = 8.43 ± 3.7 and D = 8.6 ± 2.9). Among the three groups, the time-to-peak was similar at both ROIs P and D. Conversely, the time-to-peak at the C areas was significantly longer in group A versus V (20.1 ± 13 vs. 8.43 ± 3.7; $p = 0.04$) and in group A–V versus V (20.71 ± 11.6 vs. 8.43 ± 3.7; $p = 0.03$)

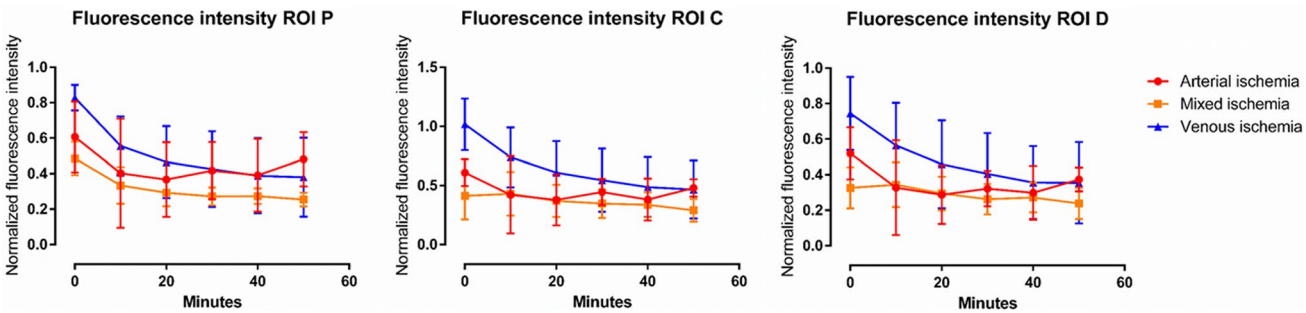

Fig. 5 Over-time evolution of fluorescence intensity (NIFU). In ROI C, after 10 min, in the A–V group the NIFU remained stable (0.43 ± 0.18), while it decreased in both the A (0.42 ± 0.32) and V (0.74 ± 0.25) groups, with a significant difference between V and AV ($p = 0.03$). Interestingly, in the A group, the signal started raising after the first 20 min of ischemia, and, after 50 min it was significantly higher than the signal observed at the same time point in the A–V group (0.48 ± 0.07 vs. 0.29 ± 0.09; $p = 0.003$). The evolution of the signal was also different at the proximal and distal ROIs. After 10 min, in the P area, the signal was significantly higher in the V (0.55 ± 0.16) when compared to the A–V group (0.33 ± 0.1; $p = 0.02$). The intensity of the signal rose proximally in the A group (0.48 ± 0.15) and the difference was statistically significant when compared to the A–V group (0.25 ± 0.04; $p = 0.005$), after 50 min. The same occurred distally, after 50 min, (A = 0.37 ± 0.06 vs. A–V = 0.23 ± 0.08; $p = 0.01$)

Discussion

FA is a promising tool to accurately document tissue perfusion in a variety of surgical applications. Large-scale multicenter trials are showing encouraging results on the impact of FA as a mean to reduce the risk of anastomotic complications [20], and randomized studies are currently underway with the aim to bring more compelling evidence [21].

However, the current setting of FA application is limited by the lack of a standardized and quantitative appreciation of the relevant fluorescence signal. There are several issues to be considered when performing FA analysis of tissue perfusion. The first one is the distance between the light source and the target: fluorescence intensity has a steep inverse relationship with the distance [10]. In other words, applied to perfusion estimation, one could obtain a relatively strong fluorescent signal in a poorly vascularized area, which

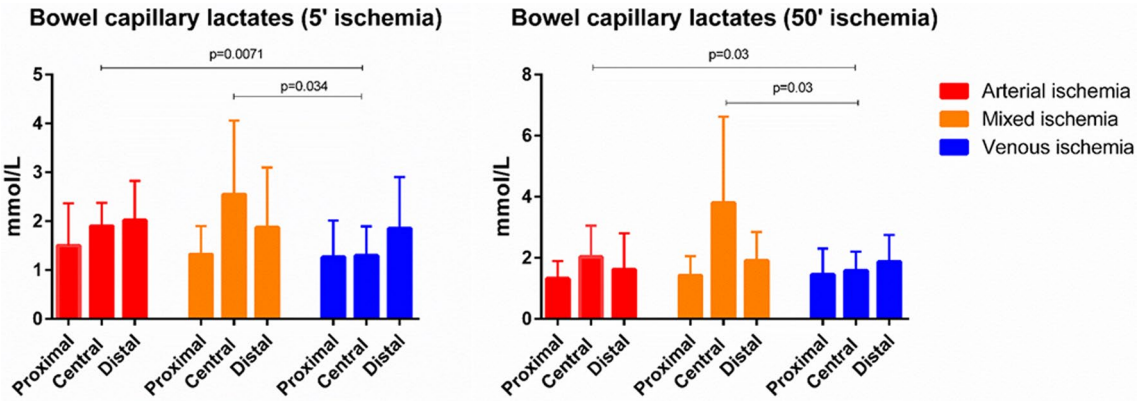

Fig. 6 Bowel local capillary lactates. After 5 min of ischemia, mean capillary lactates at the central area in the arterial and mixed ischemia group were statistically significantly higher when compared to those of the venous ischemia group, (A; 1.9 ± 0.5 and A–V; 2.6 ± 1.5 vs. V; 1.3 ± 0.6: $p = 0.0071$ and $p = 0.034$, respectively). Similarly, after 50 min of ischemia, the values remained significantly higher in the ROI C in both the arterial (2 ± 1) and mixed (3.8 ± 2.8) ischemia when compared to the venous ischemia (1.58 ± 0.6); $p = 0.03$ for both. The over-time increase of lactates was not significant, except for ROI C in the venous ischemia (1.3 ± 0.6 vs. 1.58 ± 0.6; $p = 0.049$)

is interrogated by NIR light with the camera placed very close to it and, conversely, one could have a mild fluorescent signal from a vascularized area which is observed from far away. So, in order to standardize and possibly quantify the signal, there is a need to correct by means of the distance (i.e., by utilizing a reference card providing a constant signal and, to enable reproducibility, by fixing the light source to a constant distance).

Alternatively, distance-free parameters can be used, as the dynamic evolution of the fluorescence intensity. In fact, the second important issue related to the FA, is the over-time diffusion of the fluorophore from the bloodstream to the surface of the target organs. The ICG, upon systemic injection, rapidly highlights the vessels, then diffuses quickly to the vascularized areas of the tissues but also, more slowly, to the ischemic zones.

In other words, there is an optimal window of meaningfulness of the FA, shortly after the fluorophore administration (within the first minute), after which the fluorescence signal can be detected also from ischemic areas, by capillary diffusion of the ICG, and this should be carefully considered. In order to optimize and standardize FA, there is a need for a more reliable analysis of the fluorescence signal, also enabling reproducibility between cases to obtain homogeneous data across centers.

FLER is a software-based solution that simultaneously solves both the issues related to the light source-target distance and to the dynamics of the fluorescence signal. The software elaborates a virtual perfusion cartography computing and recording the slope of the time-to-peak of fluorescence in every pixel. After being computed, the virtual cartography is superimposed onto real-time operative images to display, directly on the tissues, the dynamic of the perfusion. The FLER approach has been largely validated in the experimental setting [7–11] and is currently being translated for clinical field use [1, 22, 23].

Recently, the concept of dynamic assessment during FA, focusing the attention on the over-time evolution and on the flow speed, has been progressively applied by some groups to analyze the gastric conduit perfusion during esophagectomy [24] and rectal surgery [25]. In particular, Wada et al. have used a similar algorithm to obtain virtual perfusion cartography. In their series, including 52 low and 13 high anterior resections, FA with a side-by-side observation of virtual perfusion cartography, enabled to revise the transection line in 20% of cases [25]. In the FLER approach, the main difference is that the virtual cartography is registered on the real-time images, to obtain a mixed reality augmentation.

The software is evolving with several plug-in features, including the ability to track organs' motion to provide a constant virtual-to-real registration [26] and some ML algorithms to interpret the fluorescence signals.

In the framework of software development for FA, the hypothesis was formulated that arterial and venous ischemia have a different behavior in terms of fluorescence signal over-time evolution and that the software analysis would enable discrimination and recognition of the ischemia type.

In the present experimental study, it was possible to demonstrate that the FLER analysis can discriminate between arterial, venous and mixed ischemia, in a porcine model of colon ischemia, based on the pattern of the signal increase and wash-out.

In a nutshell, in case of venous-only ischemia, the fluorescent signal is initially brighter with a significantly shorter time-to-peak when compared to arterial and mixed ischemia.

In case of arterial ischemia, after the initial drop during the first 20 min of ischemia, the signal starts to rise again, alimented by a backflow refill of ICG (Fig. 5), which does

not occur with the other ischemia types, and that was significantly higher than the signal observed at the same time point in the A–V group.

The differences in the patterns enabled a successful application of an ML approach, despite the low sample size. The most accurate algorithms, selected with the method of the "leave-one-out cross validation", were able to discriminate between arterial and venous ischemia with 75% accuracy and up to 85% accuracy to discriminate between arterial versus mixed ischemia.

To validate the results and correlate with the imaging, the level of capillary lactates on the bowel were measured with a strip-based device. This method has been largely validated in previous studies aiming at developing the concept of metabolism-guided bowel resections [27] and to validate the concept of FLER [7–11], or to analyze regional perfusion differences after blood supply manipulation [16, 28], among others.

In the central zone of the venous ischemia, the lactates were significantly lower, immediately and 50′ after the ischemia induction, than those recorded in the arterial and mixed ischemia group.

These results are partly in contrast with the observations of Cruz et al. in a canine model of mesenteric ischemia and reperfusion (I/R) [29]. The authors aimed at comparing the changes of the regional blood flow distribution in the bowel subject to mesenteric arterial versus venous ischemia, by occlusion of the superior mesenteric artery or vein, respectively. Unlike in the present study, the bowel lactates were not directly measured, but the mesenteric vein-arterial lactate gradient, increased much more significantly after 45′ of venous ischemia, when compared to arterial ischemia. Interestingly, at the reperfusion, the lactate clearance was more pronounced in the venous group. Additionally, higher injury scores were found at the histology assessment after mesenteric venous congestion.

In a rat study, aiming at evaluating the intestinal response to different types of ischemia (arterial, venous, and arterial-venous), Guzman de la Garza et al. also identified a more marked mucosal injury and higher biological inflammatory markers in V and AV groups, when compared to the A group [30]. Similarly, in a rat model, Yano et al. found a worse histological appearance of the small bowel in the venous occlusion. However, interestingly, the maximal viability time before irreversible injuries was 2 h in the arterial occlusion model and 4 h in the venous occlusion [31].

Two additional relevant experimental studies on the rat model have been performed to evaluate the metabolic profiling of different ischemia modes. One was by Kimura et al. [32], in which the authors used the magnetic resonance spectroscopy to evaluate the intestinal metabolomic changes in venous (SMV) and arterial (SMA) I/R. The authors found that the venous occlusion induces a less severe energetic decrease, despite a longer recovery time in the reperfusion phase and, again, a worse histological score. Moreover, the arterial ischemia induced a more rapid and severe local metabolic acidosis than the venous one. Although a direct analysis of local lactate levels was not performed, such a pH change might mirror a similar behavior of lactate levels, as in the present study. The second is by Vicenti et al., in a slightly different protocol in which venous ischemia was created by portal vein (PV) occlusion. In this model, the intestinal histology injury was less pronounced following PV occlusion, most likely due to a higher oxygen and substrate availability with an increased metabolic synthetic activity, while in the SMA occlusion, higher oxidative stress was observed [33]. In a nutshell, there is an unclear physiopathology and an imbalance between tissue damage and the metabolic activity of the bowel, following different types of ischemia. A deeper physiological analysis of this issue goes beyond the scope of the rather technical aim of the present experiment.

The possibility for a real-time discrimination of the type of ischemia is particularly relevant in reconstructive and graft surgery, in which the venous outflow plays a major role in flap/graft success.

Nasser et al. could demonstrate, in an experimental rat model with various degrees of limb venous occlusion that FA can detect the presence of venous congestion early on, based on the slope of the ICG signal [34]. The authors used a software analysis to build a virtual perfusion cartography similar to the one used in this experiment, but the virtual images were displayed solely on the screen, without being overlaid on the real ones. Additionally, the authors did not compare arterial versus venous occlusion. Currently, FLER technology and a hyperspectral camera are being tested in a very similar model of limb occlusion, at our institute. Moreover, in collaboration with plastic surgeons, a porcine model of free flap for breast reconstruction has been proposed [35] and we are planning to evaluate the FLER technology in this setting.

A flap-like concept in digestive surgery is represented by the techniques of gastric tube reconstruction, in which both the impairment of the arterial blood supply and the venous congestion are considered important etiologic factors of anastomotic complications [36, 37]. The ability to intra-operatively detect a vascular compromise of the gastric conduit and to discriminate between an arterial insufficiency and a venous congestion, might lead to performing salvage procedures to improve blood flow and venous drainage. These include the technique of supercharged micro-vascular anastomosis, between short gastric vessels with cervical transverse artery and external jugular vein [38] and transient venous bloodletting to improve gastric microcirculation [39].

The minimally-invasive porcine model of colonic ischemia was selected more for practical reasons and for

the established knowledge of the model to evaluate the ability of FLER to discriminate between different types of ischemia. However, whether the intra-operative discrimination between a blood flow deficiency and a venous congestion could impact the surgical strategy in colon resections, is not known and purely speculative.

The main limitations of this study are the relatively low number of subjects, with six subjects in each ischemia group and the non-survival design. The strong points are in the methodology, and this includes the randomized design and the robustness of the validated metrics. The next sensible step is to evaluate FLER technology in the experimental flap and in gastric conduit perfusion discrimination.

In conclusion, the computer-based analysis of the fluorescence signal, including a ML approach, enables to distinguish between bowel ischemia of arterial or venous origin, with a good supervised accuracy.

Acknowledgements Authors are grateful to Christopher Burel, professional in Medical English proofreading for his assistance with the manuscript revision.

Funding This study was funded by the ARC Foundation for Cancer Research, a French foundation entirely dedicated to cancer research, in the framework of a large project (ELIOS: Endoscopic Luminescent Imaging for precision Oncologic Surgery) aiming at the development of fluorescence-guided surgery. https://www.fondation-arc.org/projets/ameliorer-diagnostic-et-traitement-chirurgical-cancers-digestifs.

Compliance with ethical standards

Disclosures Michele Diana is the recipient of the ELIOS grant from the ARC foundation. Jacques Marescaux is the President of both IRCAD and IHU-Strasbourg Institutes, which are partly funded by Karl Storz, Medtronic and Siemens Healthcare. Giuseppe Quero, Alfonso Lapergola, Manuel Barberio, Barbara Seeliger, Ines Gockel, Paola Saccomandi, Ludovica Guierriero, Didier Mutter, Alend Saadi, Marc Worreth and Vincent Agnus have no conflicts of interest or financial ties to disclose.

References

1. van Manen L, Handgraaf HJM, Diana M, Dijkstra J, Ishizawa T, Vahrmeijer AL, Mieog JSD (2018) A practical guide for the use of indocyanine green and methylene blue in fluorescence-guided abdominal surgery. J Surg Oncol 118:283–300
2. Degett TH, Andersen HS, Gogenur I (2016) Indocyanine green fluorescence angiography for intraoperative assessment of gastrointestinal anastomotic perfusion: a systematic review of clinical trials. Langenbecks Arch Surg 401:767–775
3. Blanco-Colino R, Espin-Basany E (2018) Intraoperative use of ICG fluorescence imaging to reduce the risk of anastomotic leakage in colorectal surgery: a systematic review and meta-analysis. Tech Coloproctol 22:15–23
4. Ohi M, Toiyama Y, Mohri Y, Saigusa S, Ichikawa T, Shimura T, Yasuda H, Okita Y, Yoshiyama S, Kobayashi M, Araki T, Inoue Y, Kusunoki M (2017) Prevalence of anastomotic leak and the impact of indocyanine green fluorescein imaging for evaluating blood flow in the gastric conduit following esophageal cancer surgery. Esophagus 14:351–359
5. Karampinis I, Keese M, Jakob J, Stasiunaitis V, Gerken A, Attenberger U, Post S, Kienle P, Nowak K (2018) Indocyanine green tissue angiography can reduce extended bowel resections in acute mesenteric ischemia. J Gastrointest Surg. https://doi.org/10.1007/s11605-018-3855-1
6. Liot E, Assalino M, Buchs NC, Schiltz B, Douissard J, Morel P, Ris F (2018) Does near-infrared (NIR) fluorescence angiography modify operative strategy during emergency procedures? Surg Endosc. https://doi.org/10.1007/s00464-018-6226-9
7. Diana M, Agnus V, Halvax P, Liu YY, Dallemagne B, Schlagowski AI, Geny B, Diemunsch P, Lindner V, Marescaux J (2015) Intraoperative fluorescence-based enhanced reality laparoscopic real-time imaging to assess bowel perfusion at the anastomotic site in an experimental model. Br J Surg 102:e169–e176
8. Diana M, Dallemagne B, Chung H, Nagao Y, Halvax P, Agnus V, Soler L, Lindner V, Demartines N, Diemunsch P, Geny B, Swanstrom L, Marescaux J (2014) Probe-based confocal laser endomicroscopy and fluorescence-based enhanced reality for real-time assessment of intestinal microcirculation in a porcine model of sigmoid ischemia. Surg Endosc 28:3224–3233
9. Diana M, Halvax P, Dallemagne B, Nagao Y, Diemunsch P, Charles AL, Agnus V, Soler L, Demartines N, Lindner V, Geny B, Marescaux J (2014) Real-time navigation by fluorescence-based enhanced reality for precise estimation of future anastomotic site in digestive surgery. Surg Endosc 28:3108–3118
10. Diana M, Noll E, Agnus V, Liu YY, Kong SH, Legner A, Diemunsch P, Marescaux J (2017) Reply to letter: "enhanced reality fluorescence videography to assess bowel perfusion: the cybernetic eye". Ann Surg 265:e49–e52
11. Diana M, Noll E, Diemunsch P, Dallemagne B, Benahmed MA, Agnus V, Soler L, Barry B, Namer IJ, Demartines N, Charles AL, Geny B, Marescaux J (2014) Enhanced-reality video fluorescence: a real-time assessment of intestinal viability. Ann Surg 259:700–707
12. Lee KT, Mun GH (2017) Benefits of superdrainage using SIEV in DIEP flap breast reconstruction: a systematic review and meta-analysis. Microsurgery 37:75–83
13. Fujioka M, Hayashida K, Fukui K, Ishiyama S, Saijo H, Taniguchi K (2017) Venous superdrained gastric tube pull-up procedure for hypopharyngeal and cervical esophageal reconstruction reduces postoperative anastomotic leakage and stricture. Dis Esophagus 30:1–6
14. Wang WL (2017) Venous congestion in ischemic bowel. N Engl J Med 377:e10
15. Kilkenny C, Browne W, Cuthill IC, Emerson M, Altman DG, Group NCRRGW (2010) Animal research: reporting in vivo experiments: the ARRIVE guidelines. J Gene Med 12:561–563
16. Diana M, Halvax P, Pop R, Schlagowski I, Bour G, Liu YY, Legner A, Diemunsch P, Geny B, Dallemagne B, Beaujeux R, Demartines N, Marescaux J (2015) Gastric supply manipulation to modulate ghrelin production and enhance vascularization to the cardia: proof of the concept in a porcine model. Surg Innov 22:5–14
17. Diana M, Noll E, Legner A, Kong SH, Liu YY, Schiraldi L, Marchegiani F, Bano J, Geny B, Charles AL, Dallemagne B, Lindner V, Mutter D, Diemunsch P, Marescaux J (2018) Impact of valve-less vs. standard insufflation on pneumoperitoneum volume, inflammation, and peritoneal physiology in a laparoscopic sigmoid resection experimental model. Surg Endosc 32:3215–3224
18. Pedregosa F, Gaël V, Gramfort A, Michel V, Thirion B, Grisel O, Blondel M, Prettenhofer P, Weiss R, Dubourg V, Vanderplas J, Passos A, Cournapeau D, Brucher M, Perrot M, Duchesnay É (2011) Scikit-learn: machine learning in python. J Mach Learn Res 12:2825–2830

19. Devijver PA, Kittler J (1982) Pattern recognition: a statistical approach. Prentice-Hall, London
20. Ris F, Liot E, Buchs NC, Kraus R, Ismael G, Belfontali V, Douissard J, Cunningham C, Lindsey I, Guy R, Jones O, George B, Morel P, Mortensen NJ, Hompes R, Cahill RA, Near-Infrared Anastomotic Perfusion Assessment Network V (2018) Multicentre phase II trial of near-infrared imaging in elective colorectal surgery. Br J Surg 105:1359–1367
21. Armstrong G, Croft J, Corrigan N, Brown JM, Goh V, Quirke P, Hulme C, Tolan D, Kirby A, Cahill R, O'Connell PR, Miskovic D, Coleman M, Jayne D (2018) IntAct: intra-operative fluorescence angiography to prevent anastomotic leak in rectal cancer surgery: a randomized controlled trial. Colorectal Dis. https://doi.org/10.1111/codi.14257
22. Diana M (2017) Enabling precision digestive surgery with fluorescence imaging. Transl Gastroenterol Hepatol 2:97
23. Diana M (2018) Fluorescence-guided surgery applied to the digestive system: the cybernetic eye to see the invisible. Cir Esp 96:65–68
24. Koyanagi K, Ozawa S, Oguma J, Kazuno A, Yamazaki Y, Ninomiya Y, Ochiai H, Tachimori Y (2016) Blood flow speed of the gastric conduit assessed by indocyanine green fluorescence: new predictive evaluation of anastomotic leakage after esophagectomy. Medicine (Baltimore) 95:e4386
25. Wada T, Kawada K, Takahashi R, Yoshitomi M, Hida K, Hasegawa S, Sakai Y (2017) ICG fluorescence imaging for quantitative evaluation of colonic perfusion in laparoscopic colorectal surgery. Surgical endoscopy 31:4184–4193
26. Selka F, Agnus V, Nicolau S, Bessaid A, Soler L, Marescaux J, Diana M (2014) Fluorescence-based enhanced reality for colorectal endoscopic surgery. Biomedical Image Registration, London, pp 114–123
27. Diana M, Noll E, Diemunsch P, Moussallieh FM, Namer IJ, Charles AL, Lindner V, Agnus V, Geny B, Marescaux J (2015) Metabolism-guided bowel resection: potential role and accuracy of instant capillary lactates to identify the optimal resection site. Surg Innov 22:453–461
28. Diana M, Pop R, Beaujeux R, Dallemagne B, Halvax P, Schlagowski I, Liu YY, Diemunsch P, Geny B, Lindner V, Marescaux J (2015) Embolization of arterial gastric supply in obesity (EMBARGO): an endovascular approach in the management of morbid obesity. proof of the concept in the porcine model. Obes Surg 25:550–558
29. Cruz RJ Jr, Garrido AG, Ribeiro CM, Harada T, Rocha-e-Silva M (2010) Regional blood flow distribution and oxygen metabolism during mesenteric ischemia and congestion. J Surg Res 161:54–61
30. Guzman-de la Garza FJ, Camara-Lemarroy CR, Alarcon-Galvan G, Cordero-Perez P, Munoz-Espinosa LE, Fernandez-Garza NE (2009) Different patterns of intestinal response to injury after arterial, venous or arteriovenous occlusion in rats. World J Gastroenterol 15:3901–3907
31. Yano K, Hata Y, Matsuka K, Ito O, Matsuda H (1994) Time limits for intestinal ischemia and congestion: an experimental study in rats. Ann Plast Surg 32:310–314
32. Kimura M, Kataoka M, Kuwabara Y, Sato A, Sugiura M, Fujii Y (2003) Real-time energy metabolism of intestine during arterial versus venous occlusion in the rat. J Gastroenterol 38:849–853
33. Vincenti M, Behrends M, Dang K, Park YH, Hirose R, Blasi-Ibanez A, Liu T, Serkova NJ, Niemann CU (2010) Induction of intestinal ischemia reperfusion injury by portal vein outflow occlusion in rats. J Gastroenterol 45:1103–1110
34. Nasser A, Fourman MS, Gersch RP, Phillips BT, Hsi HK, Khan SU, Gelfand MA, Dagum AB, Bui DT (2015) Utilizing indocyanine green dye angiography to detect simulated flap venous congestion in a novel experimental rat model. J Reconstr Microsurg 31:590–596
35. Bodin F, Diana M, Koutsomanis A, Robert E, Marescaux J, Bruant-Rodier C (2015) Porcine model for free-flap breast reconstruction training. J Plast Reconstr Aesthet Surg 68:1402–1409
36. Milstein DM, Ince C, Gisbertz SS, Boateng KB, Geerts BF, Hollmann MW, van Berge Henegouwen MI, Veelo DP (2016) Laser speckle contrast imaging identifies ischemic areas on gastric tube reconstructions following esophagectomy. Medicine (Baltimore) 95:e3875
37. Diana M, Hubner M, Vuilleumier H, Bize P, Denys A, Demartines N, Schafer M (2011) Redistribution of gastric blood flow by embolization of gastric arteries before esophagectomy. Ann Thorac Surg 91:1546–1551
38. Yoshimi F, Asato Y, Ikeda S, Okamoto K, Komuro Y, Imura J, Itabashi M (2006) Using the supercharge technique to additionally revascularize the gastric tube after a subtotal esophagectomy for esophageal cancer. Am J Surg 191:284–287
39. Kono K, Sugai H, Omata H, Fujii H (2007) Transient bloodletting of the short gastric vein in the reconstructed gastric tube improves gastric microcirculation during esophagectomy. World J Surg 31:780–784 (**discussion 785–786**)